International Journal of Medical Microbiology 309 (2019) 307–318

Contents lists available at ScienceDirect

International Journal of Medical Microbiology

journal homepage: www.elsevier.com/locate/ijmm

Type I interferon induced by TLR2-TLR4-MyD88-TRIF-IRF3 controls *Mycobacterium abscessus* subsp. *abscessus* persistence in murine macrophages via nitric oxide

Nanthapon Ruangkiattikul[a], Doris Rys[a], Ketema Abdissa[a], Manfred Rohde[b], Torsten Semmler[c], Pia-K. Tegtmeyer[d], Ulrich Kalinke[d], Carsten Schwarz[e], Astrid Lewin[f], Ralph Goethe[a,*]

[a] Institute for Microbiology, University of Veterinary Medicine Hannover, Hannover, Germany
[b] Central Facility for Microscopy, Helmholtz Centre for Infection Research, Braunschweig, Germany
[c] NG1 Microbial Genomics, Robert Koch Institute, Berlin, Germany
[d] Institute for Experimental Infection Research, TWINCORE, Centre for Experimental and Clinical Infection Research, A Joint Venture Between The Helmholtz Centre for Infection Research, Braunschweig, and The Hannover Medical School, Hannover, Germany
[e] Department of Pediatric Pneumonology and Immunology, Division of Cystic Fibrosis, Charité - Universitätsmedizin Berlin, Berlin, Germany
[f] FG16 Mycotic and Parasitic Agents and Mycobacteria, Robert Koch Institute, Berlin, Germany

ARTICLE INFO

Keywords:
Interferon-β
Non-tuberculous mycobacteria
Inducible nitric oxide synthase
Macrophage
Bacterial clearance
Cystic fibrosis

ABSTRACT

Mycobacterium abscessus (MAB) is an emerging, rapidly growing non-tuberculous *Mycobacterium* causing therapy-resistant pulmonary disease especially in patients with cystic fibrosis (CF). Smooth and rough colony type MAB can be isolated from infected patients whereby rough colony type MAB are more often associated with severe disease. Disease severity is also associated with an alternated type I interferon (IFN-I) response of the MAB-infected patients. However the relevance of this response for the outcome of MAB infection is still unknown. In this study, we analyzed the IFNβ expression of murine macrophages infected with a MAB rough colony strain (MAB-R) isolated from a patient with progressive CF and compared it to macrophages infected with the MAB smooth colony type reference strain (MAB-S). We found that MAB-R infected macrophages expressed significantly more IFNβ mRNA and protein than MAB-S infected macrophages. Higher IFNβ induction by MAB-R was associated with higher TNF expression and intracellular killing while low IFNβ induction was associated with lower TNF expression and persistence of MAB-S. IFNβ induction was independent of the intracellular cGAS-STING recognition pathway. MAB appeared to be recognized extracellularly and induced IFNβ expression via TLR2-TLR4-MyD88-TRIF-IRF3 dependent pathways. By using macrophages lacking the IFN-I receptor we demonstrate that MAB induced IFN-I response essentially contributed to restricting MAB-R and MAB-S infections by activating macrophage *Nos2* expression and nitric oxide production. Thus IFN-I seem to influence the intrinsic ability of macrophages to control MAB infections. As MAB persists over long time periods in susceptible patients, our findings suggest that virulence of MAB strains is promoted by an insufficient IFN-I response of the host.

1. Introduction

Incidence and prevalence of lung disease caused by non-tuberculous mycobacteria (NTM) such as the members of the *Mycobacterium* (*M.*) *avium* complex and the *M. abscessus* complex (MABC) are increasing worldwide (Kim et al., 2015b; Wassilew et al., 2016). The MABC comprises three subspecies, *Mycobacterium abscessus* subsp. *abscessus* (MABa), *Mycobacterium abscessus* subsp. *massiliense* (MABm) and *Mycobacterium abscessus* subsp. *bollettii* (MABb) (Lee et al., 2015). Among those MABa is the most common subspecies isolated from patients. MABa causes a wide range of infections including skin and soft tissue infections and is often isolated from patients with chronic obstructive lung disorders such as cystic fibrosis (CF) (Pawlik et al., 2013; Ruger et al., 2014). A more recent population study on CF patients revealed that worldwide distributed, transmissible and genetically closely related MAB strains were associated with severe clinical outcomes (Bryant et al., 2016).

MAB virulence is associated with the morphological switch from smooth to rough colony types (S-type, R-type). Such conversion appears to arise during infection in the host triggered by antibiotic treatments

* Corresponding author at: Institute for Microbiology, University of Veterinary Medicine Hannover, Bischofsholer Damm 15, 30173, Hannover, Germany.
E-mail address: ralph.goethe@tiho-hannover.de (R. Goethe).

https://doi.org/10.1016/j.ijmm.2019.05.007
Received 21 December 2018; Received in revised form 8 April 2019; Accepted 31 May 2019

(Tsai et al., 2015). The major difference between these two colony types is the loss of glycopeptidolipids (GPL) in the R-type (Howard et al., 2006) leading to an irregular dry surface with wrinkles and crest colony, cellular aggregation and cord forming morphology (Nessar et al., 2011). The S-type is characterized by moist texture and bright colony color, bacterial motility and biofilm formation (Jonsson et al., 2007; Nessar et al., 2011). S-type MAB is commonly isolated from wound infection and sporadically from lung infections. It is suggested to exhibit some of the virulence traits present in slow growing mycobacterial pathogens such as *M. tuberculosis* or *M. avium*. Hence, it can restrict phagosomal acidification, but does not multiply in macrophages. Its capacity to induce apoptosis and autophagy is weak (Roux et al., 2016). In contrast, the R-type MAB has been shown to multiply in human monocytes and is often isolated from lung infections (Byrd and Lyons, 1999). This phenotype is characterized by a hyper-proinflammatory response (TNF, IL12, IFNγ) via Toll-like receptor (TLR) 2 signaling (Howard et al., 2006; Kim et al., 2015a; Rhoades et al., 2009; Roux et al., 2011). Both colony types are found in the clinical specimens of CF patients, however, the R-type MABa are predominantly isolated (Pawlik et al., 2013; Ruger et al., 2014).

Type I interferons (IFN-I) such as IFNβ and IFNα compromise a group of cytokines involved in various inflammatory reactions during infection and cancer (Borden et al., 2007). IFN-I expression is activated though interaction of pathogen associated molecular patterns (PAMP) with membrane-bound pattern recognition receptors (PRR). Toll-like receptors (TLR) are one family of PRR, which includes plasma membrane located TLR2 and TLR4 as well as endosomal membranes located TLR3, TLR7 and TLR9. Activation of these receptors results in a MyD88/TRIF-dependent IFN-I induction. Alternatively, cytosolic PAMP can induce IFN-I responses via cytosolic PRR, such as cyclic GMP-AMP synthase (cGAS). Extracellular bacterial DNA released from bacteria (eDNA) binds to cytosolic cGAS, leading to synthesis of cyclic GMP-AMP (cGAMP). cGAMP activates the STING-TBK-1-IRF3 signaling pathway to initiate transcription of *Ifnb* (Andrade et al., 2016; Hansen et al., 2014; Ruangkiattikul et al., 2017; Watson et al., 2015). All IFN-I signal via the heteromeric IFN-I receptor (IFNAR) and act locally and systemically to coordinate diverse responses to infection. The protective role of IFN-I in viral infections is well known (Trinchieri, 2010). However, in bacterial infection the role of IFN-I can be either beneficial or detrimental depending on the bacterial species and the route of infection (Boxx and Cheng, 2016; Denis, 1991; Kuchtey et al., 2006; Ruangkiattikul et al., 2017).

IFN-I are important for lung inflammatory responses of the host (Makris et al., 2017). Increasing evidence suggests that IFN-I signaling is involved in the host defense against NTM infection (Denis, 1991; Frau et al., 2015; Ruangkiattikul et al., 2017). Moreover, IFN-I seem to play an important role in bacterial control in CF. In epithelial cells with cystic fibrosis transmembrane conductance regulator (CFTR) mutation, the cause of CF disease, the production of IFN-I was abrogated and the cells showed an impaired bacterial clearance (Parker et al., 2012). Furthermore, IFN-I induced gene expression was related to patients with mild forms of CF (Kormann et al., 2017). This is most likely because IFN-I with the help of other cytokines such as TNF activates inducible nitric oxide synthase 2 (NOS2) and nitric-oxide (NO) production (Bogdan, 2015; Costa et al., 2006; Dietrich et al., 2010; Huys et al., 2009; Jacobs and Ignarro, 2001; Pahari et al., 2016). NO is considered to be the major effector molecule in controlling bacterial infection (Pahari et al., 2016; Yang et al., 2016; Zwaferink et al., 2008). Depending on the dose, NO can either kill bacteria or restrain bacterial replication by inducing mycobacterial dormancy (Chan et al., 2001; Pacl et al., 2018; Voskuil et al., 2003). Air way epithelial cells of CF patients express low levels of *Nos2* (Moeller et al., 2006). Accordingly, inhalation of NO has been shown to be a very effective method for bacterial clearance in CF patients (Yaacoby-Bianu et al., 2018).

There is still no conclusive evidence for the role of IFN-I in NTM infections and even less is known for MAB infections. Different signaling pathways have been described to activate IFN-I production in mycobacteria infected macrophages. For instance, the release of eDNA from intracellular bacteria triggers cGAS-STING dependent IFN-I induction in *M. tuberculosis* infected macrophages (Manzanillo et al., 2012; Watson et al., 2015). Nevertheless, TLR2 and TLR4 signaling also seems to contribute to the IFN-I induction (Carmona et al., 2013; Jang et al., 2018). We have recently shown that IFN-I induced by intracellular bacterial eDNA and the cGAS-STING pathway is required to restrict NTM infection (Ruangkiattikul et al., 2017). In the present study, we examined the role of IFN-I upon infection of macrophages with MAB R-type and S-type strains. Using murine bone marrow derived macrophages we found that the MAB R-type strain and the MAB S-type strain induced *Ifnb* to different extents. In contrast to our previous findings the induction was not activated via the cGAS-STING pathway, but exclusively by the activation of TLR2-TLR4-MyD88-TRIF-IRF3 signaling. We show that the extent of macrophage IFN-I responses is directly linked to an autoregulatory *Nos2* induction and antimicrobial NO production influencing MAB survival in macrophages.

2. Material and methods

2.1. Isolation of MABa CF34/14-1 from sputum

Strain MABa CF34/14-1 (rough colony variant) was isolated in a study approved by the ethics committee of the Charité – Universitätsmedizin Berlin (EA2/093/12) from sputum of a 28 years old patient with progressive CF homozygous for the F508del mutation. At isolation time the FEV1 was 46% predicted, BMI 19.5 kg/m^2. The patient suffered from chronic pan-sinusitis, pancreatic insufficiency, CF-related diabetes mellitus and chronic colonization with *Pseudomonas aeruginosa*. The CT scan showed bronchiectasis of the right lung and complete atelectasis of the left lung with consecutive mediastinal shift to the left.

One ml sputum was decontaminated with an equal volume of 0.25% N-acetyl-L-cysteine and 1% sodium hydroxide (NALC-NaOH). After addition of NALC-NAOH the sample was mixed and incubated for 10 min at room temperature (RT). Then water was added to a volume of 40 ml and the sample was centrifuged to collect the bacterial pellet, which was resuspended in 1 ml of sterile water. Dilutions were plated on Middlebrook (MB) 7H11 agar plates supplemented with 10% OADC (Becton Dickinson) and 0.5% glycerol. Cycloheximide (5%) was added to suppress fungal growth. After several days rough colonies appeared and were picked on agar and colony material from the plates was heated for 30 min at 97 °C. The supernatants were used to perform the genus-specific PCR with primers 16S rRNA F/R as described (Shin et al., 2010) and Mabs species-specific duplex-PCR with the primers Mab1 F/R and Mab2 F/R described in Choi et al. (Choi et al., 2011). Confirmation of assignment to MABa was obtained by performing PCR with the primers 16SrDNA-FW (5′-TGGAGAGTTTGATCCTGGCTCAG-3′) and 16SrDNA-Rev (5′-TGCACACAGGCCACAAGGGA-3′), sequencing the 1030 bp product and performing Blast analysis. The subspecies was determined by phylogenetic analysis of the whole genome sequence of the strain as described below.

2.2. Other bacterial strains and growth conditions

M. smegmatis mc^{2}155 (ATCC 19420) has been described (Kuehnel et al., 2001). *M. abscessus* subsp. *abscessus* DSM 44196 smooth colony variant (MAB-S, ATCC 19977: reference strain) and strain CF34/14-1 (MAB-R) were grown in MB 7H9 medium or on solid MB 7H10 agar plates (for *M. smegmatis*) and MB 7H11 agar plates (for *M. abscessus*) (Beckton Dickinson) supplemented with 10% ADC (5% albumin/2%

glucose/145.45 mM NaCl) and 0.2% and 0.5% glycerol for the preparation of broth or agar respectively. Bacteria were grown in MB broth containing 0.025% tyloxapol (Sigma) to early-log phase (OD_{600} of 0.8 and 1.8 for MAB-S and MAB-R respectively), washed two times with PBS (Sigma), and re-suspended in 10% glycerol (Roth) in MB broth. Bacteria were vortexed in the presence of 2.85–3.45 mm glass beads (Roth) for 5 min and centrifuged at 50xg for 5 min. Supernatant containing prevalently single mycobacteria was frozen at -20°C. One week before each experiment, individual tubes were thawed and titrated to determine CFU. For the growth characteristic, bacteria were cultured at an initial OD_{600} of 0.025. Stirring cultures were grown at 37°C at 130 rpm for 7 days, the optical density detected at OD_{600} was determined.

2.3. Next generation sequencing and bioinformatics analysis

DNA from strain MABa CF34/14-1 was isolated as described in (Coscolla et al., 2013) and used for whole genome sequencing. Libraries for Illumina short read sequencing were prepared from 1 ng of extracted DNA utilizing the Nextera XT DNA Library Prep Kit according to the manufacturer's recommendations (Illumina Inc., USA). Sequencing was carried out in paired-end (2 × 250 bp) on a HiSeq 1500 instrument running the rapid mode and generating an amount of data that guaranteed a coverage > 90x per genome. FastQ files from the sequencer and from the European Nucleotide Archive of EMBL-EBI for the genomes from Bryant et al. (2016) were adapter- and barcode-trimmed by running flexbar v3.3.0 (Roehr et al., 2017) and then assembled into contiguous sequences by using SPAdes v3.11.0 (Bankevich et al., 2012). The draft genomes were provided as an input into the ROARY Pan-genome pipeline v3.11.2 (Page et al., 2015) or generating an alignment of orthologous genes. Based on this alignment a Maximum Likelihood phylogeny of the genomes was calculated with RAxML v8.2.9 (Stamatakis, 2014).

2.4. Macrophage culture and infection

Bone marrow cells were isolated from the bones of C57BL/6 wild-type, cGAS$^{-/-}$, TLR2$^{-/-}$, MyD88$^{-/-}$, IRF3$^{-/-}$, IFNAR$^{-/-}$, STING$^{-/-}$, TRIF$^{-/-}$, UNC93B$^{-/-}$, and transgenic IFN-β luciferase reporter mice (IFN-β$^{+/\Delta\beta\text{-luc}}$) as described earlier (Ruangkiattikul et al., 2017). Bones of NOS2$^{-/-}$ C57BL/6 mice and TLR4$^{-/-}$ C57BL/10ScNJ mice were obtained from the breeding facility of the Universitätsklinikum Erlangen. Cells were cultured in IMEM medium (Thermo Fisher) supplemented with 10% FCS (Biochrom), 1% glutamine (Thermo Fisher), 100 units/ml penicillin, 100 µg/ml streptomycin (Thermo Fisher) in the presence of 20% L929-cell conditioned medium for 10 days. For infection experiments, macrophages were cultured in antibiotic free IMDM (Thermo Fisher) supplemented with 10% FCS, 1% glutamine overnight and infected with a suspension containing mostly single mycobacteria at MOI of 10. After 1 h incubation, BMDM were washed 2 times with PBS and IMDM containing 200 µg/ml amikacin (MP Biomedicals) was added to inhibit remaining extracellular bacteria. After 2 h incubation, antibiotic free medium was replaced. Cells were incubated until the desired time periods. For phagocytosis inhibition studies, 5 µM latrunculin B (Calbiochem) was added 1 h prior to the addition of bacteria and included throughout the experiment. PAM_2CSK_4 (Invivogen), LPS (Invivogen) and *M. smegmatis* were used as a positive control in TLR2, TLR4 and cGAS-STING experiments, respectively.

2.5. Intracellular cytokine staining

BMDM were fixed and permeabilized using fixation and permeabilization buffers (eBioscience) according to the manufacturer's instructions. Cells were stained with anti-TNFα-APC (Miltenyi Biotec) and subjected to flow cytometric analysis.

2.6. Association and internalization and in vitro intracellular bacterial survival assay

For bacterial association with macrophages, BMDM were infected with MAB-R or MAB-S at MOI of 10. At 1 h post infection (p.i.), BMDM were washed 2 times with cold PBS, lysed with PBS containing 1% NP40 (Roche diagnostics) and passaged through a 24-gauge needle. Cells were serially diluted and plated on LB agar. Percentage of association was calculated by relating the number of bacteria plated at 1 h p.i. to the initial bacterial inoculum used for infection. For internalization, infected BMDM at 1 h p.i. were washed 2 times with PBS and incubated for 1 h with IMDM containing 200 µg/ml amikacin (MB biomedicals) and processed as mentioned above. Internalization was expressed as the percentage of intracellular bacteria at 2 h p.i. relative to the initial inoculum. For intracellular bacterial survival assay, cells were harvested at 2 h, 24 h, 48 h and 72 h and processed as mentioned above. The numbers of bacteria at 2 h p.i. representing intracellular bacteria was set to 100%. Intracellular bacteria at 24 h, 48 h and 72 h were calculated as percentage referring to 2 h p.i.

2.7. RNA extraction and qRT-PCR

RNA was extracted and reverse transcribed using M-MLV reverse transcriptase (Promega) as described by the manufacturer. qRT-PCR was performed using a Mx3005 P qPCR system (Agilent Technologies). Ct values were normalized to the housekeeping gene *Rps9* (Δct) and expressed as fold change to the untreated control (ΔΔct). Primer sequences are shown as 5′-3′. *Rps9*_fw: CTGGACGAGGGCAAGATGAAGC. *Rps9*_rv: TGACGTTGGCGGATGAGCACA. *Ifnb*_fw: ACCACAGCCCTCTC CATCAACTA. *Ifnb*_rv: CTCTTCTGCATCTTCCTCCGTCATC. *Ip10*_fw: GTGTTGAGATCATTGCCACGA. *Ip10*_rv: GCTTACAGTACAGAGCTAGG. *Nos2*_fw: GGCTGTCAGAGCCTCGTGGCTTTGG. *Nos2*_rv: CCCTTCCGAA GTTTCTGGCAGCAGC. *Tnf*_fw: ATGAGCACAGAAAGCATGATC. *Tnf*_rv: TACAGGCTTGTCACTCGAATT.

2.8. Immunoblot analysis

Cells were lysed in cell extraction buffer (Thermo Fisher) supplemented with 1x protease inhibitor cocktail P8340 (Thermo Fisher), 0.5 mM AEBSF (CalBiochem) and 1x Halt phosphatase inhibitor cocktail (Thermo Fisher). Cell lysates were separated by 12.5% SDS-PAGE and transferred onto nitrocellulose membranes. Blots were incubated with anti phospho-TBK1/NAK (Ser172, D52C2) and anti GAPDH (Cell Signalling) antibodies.

2.9. Nitric oxide production

Cell culture supernatants were collected from infected BMDM cells at 48 h and 72 h. NO was estimated by Griess method (Invitrogen) according to manufacturer' instructions with a minor modification. Briefly, supernatants (150 µl) were incubated with 50 µl of Griess component B (10 mg/ml sulfanilic acid) for 10 min at RT in the dark. Later, 50 µl component A (1 mg/ml *N*-(1-naphthyl) ethylenediamine dihydrochloride) was added followed by 10 min incubation at RT in the dark. Absorbance was measured at 548 nm and the nitrite concentration was calculated based on the standard curve.

2.10. ELISA

Cell culture supernatants were collected from infected BMDM cells at 8 h and 24 h. IFNβ was analyzed using LumiKine™ Xpress mIFN-β ELISA kit following the manufacturer's instruction (Invivogen).

2.11. Field emission scanning electron microscopy

Infected cells on glass cover slips were fixed at the indicated time

points with 2% glutaraldehyde and 5% formaldehyde in HEPES buffer (0.1 M HEPES, 10 mM CaCl2, 10 mM MgCl2 and 0.09 M sucrose, ph 6.9). Fixative was removed by washing twice in TE-buffer (20 mM TRIS, 2 mM EDTA, pH 7,0) before dehydrating in a graded series of acetone (10, 30, 50, 70, 90, 100%) on ice for 10 min for each step. Samples in 100% acetone were allowed to reach room temperature before another change of 100% acetone. Samples were then subjected to critical-point drying with liquid CO_2 (CPD 030, Bal-Tec, Liechtenstein). Dried samples were covered with a gold-palladium film by sputter coating (SCD 500 Bal-Tec, Liechtenstein) before examination in a field emission scanning electron microscope Zeiss Merlin (Carl Zeiss, Oberkochen) using the Everhart Thornley SE-detector and the inlens-SE detector in a 50:50 ratio with an acceleration voltage of 5 kV. Contrast and brightness were adjusted with Adobe Photoshop CS5.

2.12. Ultrathin sections and transmission electron microscopy

Infected cells grown on plastic were fixed with 2% glutaraldehyde and 5% formaldehyde in HEPES buffer, scratched from the plastic, washed twice with TE buffer and then osmificated with 1% aqueous osmium for one hour at room temperature. Samples were then embedded into 2% water agar, dehydrated with a graded series of acetone (10%, 30%, 50%, 70%, 90%, and 100%) for 30 min at each step. Dehydration in 70% acetone was done with 2% uranyl acetate overnight. Samples were then infiltrated with epoxy low viscosity resin (1 part acetone/1 part resin; 1 part acetone/2 parts resin, pure resin alternating) following the hard formular. Ultrathin sections were cut with a diamond knife, picked up with butvar-coated grids and counterstained with 4% aqueous uranyl acetate. Samples were examined in a TEM910 transmission electron microscope (Carl Zeiss, Oberkochen) at an acceleration voltage of 80 kV. Images were taken at calibrated magnifications using a line replica. Images were recorded digitally with a Slow-Scan CCD-Camera (ProScan, 1024 × 1024, Scheuring, Germany) with ITEM-Software (Olympus Soft Imaging Solutions, Münster, Germany). Contrast and brightness were adjusted with Adobe Photoshop CS5.

2.13. Statistical analysis

Data are expressed as means ± SEM by using GraphPad Prism 7.0 (GraphPad, San Diego, CA, USA). Depending on the experiment, two tailed Student's *t*-test and one-way ANOVA with Tukey post test were used. The difference between samples and controls was considered statistically significant at a level of $^{*}p < 0.05$, $^{**}p < 0.01$ and $^{***}p < 0.001$.

3. Results

3.1. MAB-R exhibits slower growth and higher internalization rate than MAB-S, but is unable to establish a persistent infection in macrophages

To analyze IFN-I expression of MABa infected macrophages, we used a MABa clinical isolate from a patient with cystic fibrosis that shows a stable rough and dry colony morphotype (CF34/14-1, following designated as MAB-R) and the MABa reference strain with smooth and moist colony morphotype (ATCC 19977, following designated as MAB-S) (Fig. 1A, upper panel). Whole genome comparison (Fig. 1B) revealed that MAB-R (CF34/14-1) belongs to cluster 2 of the two world-wide distributed MABa clusters that are considered to be transmissible between patients and particularly virulent (Bryant et al., 2016). Comparison of genes involved in gpl synthesis from strain ATCC 19977 (GeneBank accessions AM231618 and AM231619) and CF34/14_1 (GeneBank accession RRCG00000000) revealed non-synonymous mutations in genes *atf2*, *atf1*, *gtf2*, *fmt*, *mps1*, *mps2*, *fadD28*, *papA3,* and *pks* explaining the rough phenotype of isolate CF34/14_1.

As MAB-R tended to form clumps in the culture, we established a technique to culture both strains as single cell suspensions to obtain comparable results on the outcomes of macrophage infection. This was obtained by culturing MAB-R and MAB-S in stirring MB broth cultures in the presence of 0.025% tyloxapol. Phase contrast microscopic pictures of MAB-R and MAB-S revealed that both strains grew as single cell suspensions (Fig. 1A, lower panel). The growth kinetics revealed that MAB-R entered early log phase at 30 h and reached the stationary phase

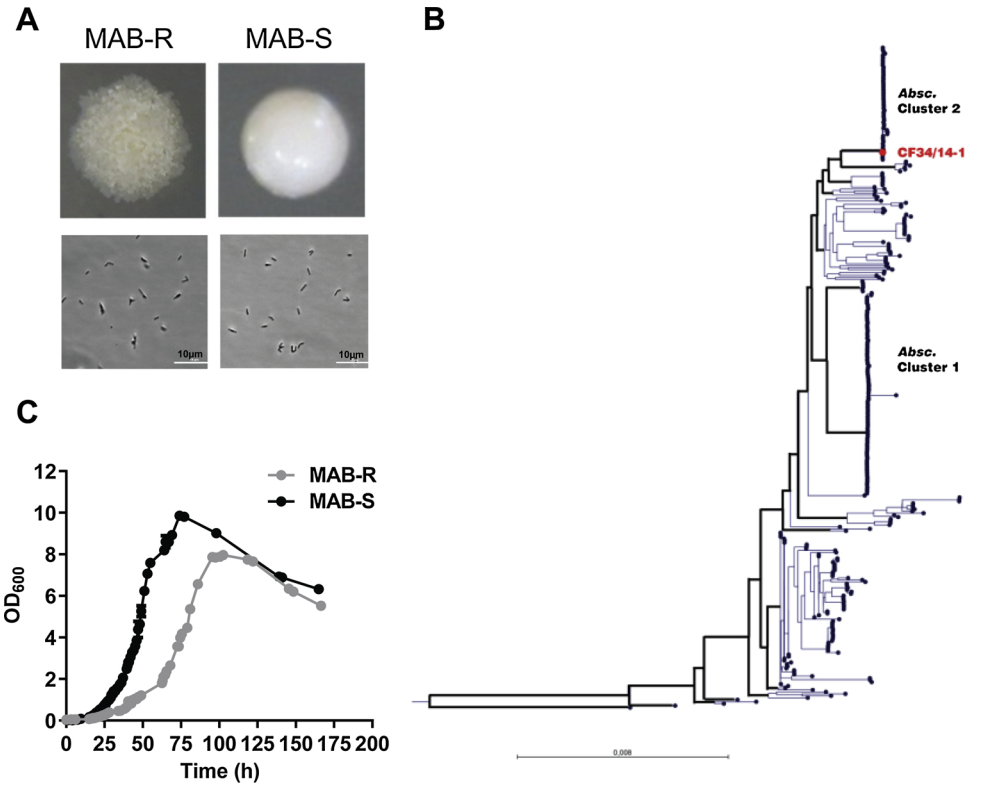

Fig. 1. General characteristics of MAB-R and MAB-S. (A upper panel) Colonies of MAB-R and MAB-S grown on MB M7H11 agar. (A lower panel) Phase contrast microscopy and differential interference contrast images of MAB-R and MAB-S stirring culture grown in MB broth. The scale bar represents 10 µm. (B) Maximum Likelihood Phylogeny of 337 *M. abscessus* genomes from the study of Bryant et al. (2016) and MABa genome of CF34/14-1 from this study marked in red. The basis for the calculation were 3,755 orthologous genes that form the maximum common genome for this set of strains. An enlarged version of the tree can be found as Fig. S1. (C) Growth of MAB-R, MAB-S stirring cultures containing 0.025% tyloxapol (For interpretation of the references to colour in this figure legend, the reader is referred to the web version of this article).

by 90 h. MAB-S showed faster growth compared to MAB-R. It needed 15 h and 75 h to reach early log phase and stationary phase, respectively (Fig. 1C). To investigate whether the so grown bacteria behave differently regarding association to, internalization by, and survival in macrophages, BMDM were infected with MAB-R and MAB-S of early log phase at MOI of 10. Interestingly, when bacteria were added into the infection medium (IMDM) on macrophage monolayer, MAB-R spontaneously aggregated to clumps containing multiple bacteria while most of MAB-S were single or organised in small clumps with 2–4 bacilli (Fig. 2 A–D). As a result, macrophage phagocytosed cell rich clumps of MAB-R and small clumps cells of MAB-S. We never observed single bacteria containing vaculoes in MAB-S infected macrophages. Monitoring macrophage cell death by propidium iodid (PI) staining revealed that viability of macrophages was not influenced by the up-take of MAB-R clumps (Fig. S3).

Next, we determined the numbers of macrophage associated and intracellular bacteria by CFU plating. To get rid of extracellular bacteria in survival assays, 1 h after infection BMDM were washed and incubated with cell culture medium containing 200 µg/ml amikacin for 2 h. This treatment resulted in less than 1% of extracellular bacteria in the cell culture supernatants when compared to the initial bacteria added at time 0 (Fig. S2). As shown in Fig. 2E, both bacterial strains showed similar associations with macrophages (CFU of adherent and intracellular bacteria after 1 h of macrophage infection). As expected from the electron micrographs the number of internalized MAB-R appeared higher (CFU of bacteria after 1 h of macrophage infection and 1 h of amikacin treatment) than internalized MAB-S (Fig. 2F). Next, we investigated bacterial persistence. For this, due to the different internalization rate, the number of intracellular bacteria at the indicated times was referred to 2 h p.i. which was set to 100%. As shown in Fig. 2G, MAB-R was unable to survive inside macrophages while MAB-S was able to survive and to moderately replicate intracellularly.

3.2. Induction of Ifnb expression of M. abscessus infected macrophages is colony morphotype dependent

We have previously shown that pathogenic NTM, *M. avium* ssp. *paratuberculosis*, which is able to survive in macrophages induce poor IFN-I expression whereas nonpathogenic NTM, *M. smegmatis,* which is killed by the macrophages is a strong inducer of IFN-I (Ruangkiattikul et al., 2017). To prove if the same situation applies in MAB infection, we infected BMDM expressing the luciferase gene under the control of the *Ifnb* promoter (Lienenklaus et al., 2009) with MAB-R and MAB-S and determined luciferase activity after 4 h and 8 h. As shown in Fig. 3A, MAB-R infection induced luciferase expression in macrophages after 4 h and expression dropped after 8 h. By contrast, the induction in MAB-S infected macrophages was significantly weaker. Next, we monitored the kinetics of *Ifnb* by qRT-PCR. *Ifnb* expression was induced and reached its peak at 60-folds by 4 h after infection of macrophages with MAB-R, while *Ifnb* expression was significantly lower in MAB-S infected macrophages (Fig. 3B). In agreement, we found differential amounts of IFN-β protein in the supernatants of infected BMDM (Fig. 3C) and the expression of *Ip10*, an IFN-I inducible gene (Fig. 3D), followed *Ifnb* expression. TNF has been shown to be strongly induced by R-type MAB in human monocyte derived macrophages (Rhoades et al., 2009). As shown in Fig. 3E and F, strong *Tnf* induction occurred in MAB-R infected BMDM whereas *Tnf* was weakly up-regulated in MAB-S infected BMDM. Overall, the results clearly show differential activation of macrophage inflammatory cytokines in response to MAB-R and MAB-S infections.

3.3. M. abscessus induced Ifnb expression does not depend on cytosolic and intracellular signaling

Our recent works showed that induction of *Ifnb* expression by *M. smegmatis* depended on differential eDNA release and signaling via cGAS-STING-TBK1-IRF3 axis (Ruangkiattikul et al., 2017). Hence, we were interested whether the same pathway is involved in *Ifnb* production in macrophages infected with MAB-R and MAB-S. By immunoblot analysis we found that phosphorylation of TBK1 was strongly enhanced in macrophages infected with MAB-R, but not with MAB-S (Fig. 4A). In addition, *Ifnb* expression was significantly reduced in IRF3$^{-/-}$ macrophages infected with both strains (Fig. 4B). Surprisingly, *Ifnb* expression induced by MAB-R and MAB-S was not reduced in BMDM from mice lacking cGAS or STING, while the IFNβ expression after *M. smegmatis* (MSM) infection, which is known to be recognized by cGAS-STING via eDNA release (Ruangkiattikul et al., 2017), was diminished (Fig. 4C). In addition, there was also no significant difference of *Ifnb* expression in BMDM lacking the TLR3, 7, 9 adaptor protein UNC93B (UNC93B$^{-/-}$) in response to both strains (Fig. 4D), excluding intracellular TLR as sensors of MAB-R and MAB-S. Thus, MAB infection of macrophages is recognized independent of cGAS-STING and the intracellular TLR3, 7, and 9. This is remarkable as MAB infection of macrophages triggers a different sensing pathway than other mycobacterial infections.

3.4. TLR2-TLR4-MYD88-TRIF signaling is necessary for M. abcessus induced Ifnb expression

The above described findings raised the question which pathway activates TBK1-IRF3 signaling in MAB infected macrophages. To dissect the signaling pathway we infected MyD88$^{-/-}$ and TRIF$^{-/-}$ macrophages with MAB-R or MAB-S. As shown in Fig. 5A, *Ifnb* expression was significantly reduced in MAB-R infected MyD88$^{-/-}$ and TRIF$^{-/-}$ macrophages compared to infected wild-type macrophages. A tendency of lower expression in MyD88$^{-/-}$ and TRIF$^{-/-}$ macrophages was observed in the MAB-S infected groups. As mycobacteria are preferentially recognized by TLR2, we analyzed *Ifnb* expression in WT and TLR2$^{-/-}$ macrophages infected with MAB-R or MAB-S. As shown in Fig. 5B, absence of TLR2 significantly reduced *Ifnb* expression of MAB-R infected macrophages as well as of macrophages treated with the TLR2 ligand PAM_2CSK_4 that was included as a control. The result indicated the involvement of TLR2 signaling in MAB induced *Ifnb* expression. Since TLR2 induced *Ifnb* expression via TBK1-IRF-3 is rather untypical and only described to occur after TLR2 receptor internalization we pretreated BMDM with latrunculin B for 1 h to block bacterial uptake before MAB infections. In these experiments, we included MSM which is known to activate *Ifnb* expression only if it is taken up by the macrophage (Ruangkiattikul et al., 2017). As expected, latrunculin B treatment significantly reduced *Ifnb* expression of MSM infected macrophages (Fig. 5C). However, *Ifnb* expression was not altered in MAB infected macrophages after latrunculin B pre-treatment, indicating that *Ifnb* expression in MAB infected macrophages was induced from the macrophage's surface (Fig. 5C). TLR4 signaling has been described to be involved in IFNβ induction in MTB (Jang et al., 2018). Therefore, to explain TRIF-dependency of MAB-R induced *Ifnb* expression, we infected TLR4$^{-/-}$ macrophages. As shown in Fig. 5D, in the absence of TRL4 MAB induced *Ifnb* expression was completely abolished. In addition, we found that viability of bacteria was not necessary for *Ifnb* induction by MAB as heat-inactivated bacteria could stimulate the same level of *Ifnb* expression (Fig. 5E). This indicates that heat stable structural mycobacterial components are responsible for TLR4 mediated IFNβ induction. Taken together, our data clearly demonstrate that MAB-R and MAP-S activate IFNβ production via TLR2-TLR4-IRF3 pathway, most probably by using MyD88 and TRIF as adaptor molecules.

3.5. IFN-I dependent NO production is necessary to control MAB survival in macrophages

IFN-I is known to be a strong co-inducer of NO production (Bachmann et al., 2017; Dietrich et al., 2010; Pahari et al., 2016). To

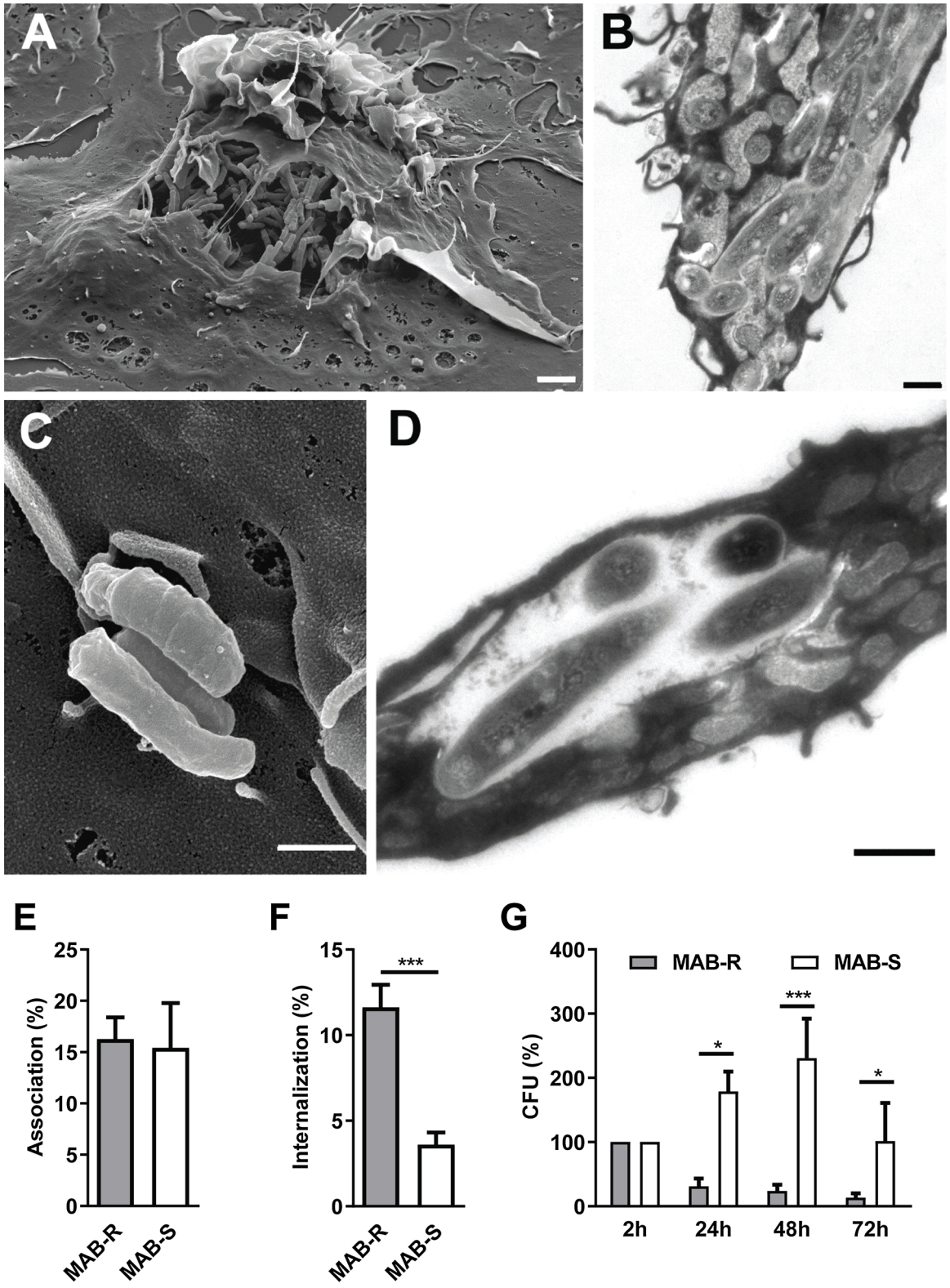

Fig. 2. Macrophage interactions of MAB-R and MAB-S. Upper panel of images: Scanning electron microscopy images showing the interaction of macrophages with MAB-R (A) and MAB-S (C) 30 min after infection of BMDM with both strain at MOI of 10, and transmission electron microscopy images of BMDM infected with MAB-R (B) and MAB-S (D) for 2 h at MOI of 10. Bars represent: A = 2 μm, B–D = 0.5 μm, E = 2 μm. Lower panel: (E) Percentage of bacteria- macrophages association. BMDM were infected with MAB-R or MAB-S for 1 h. Cells were lysed and plated and the percentage of adherent bacteria was calculated referring to the initial inoculum. (F) Percentage of intracellular bacteria. BMDM were infected with MAB-R or MAB-S for 1 h. Cells were then cultured in IMDM medium containing 200 μg/ml amikacin for 1 h. BMDM were lysed and plated and the intracellular bacteria were calculated referring to the initial inoculum. (G) Intracellular survival of MAB-R and MAB-S. BMDM were infected with MAB-R or MAB-S at MOI of 10 for 1 h. Bacteria were washed and medium containing 200 μg/ml amikacin was added for 2 h. Intracellular bacteria were plated at indicated time points. The percentage was referred to 2 h p.i. set as 100%. Data are presented as mean ± SEM from at least 3 independent experiments, *$p < 0.05$, ***$p < 0.001$ by 2 tailed Student's *t*-test.

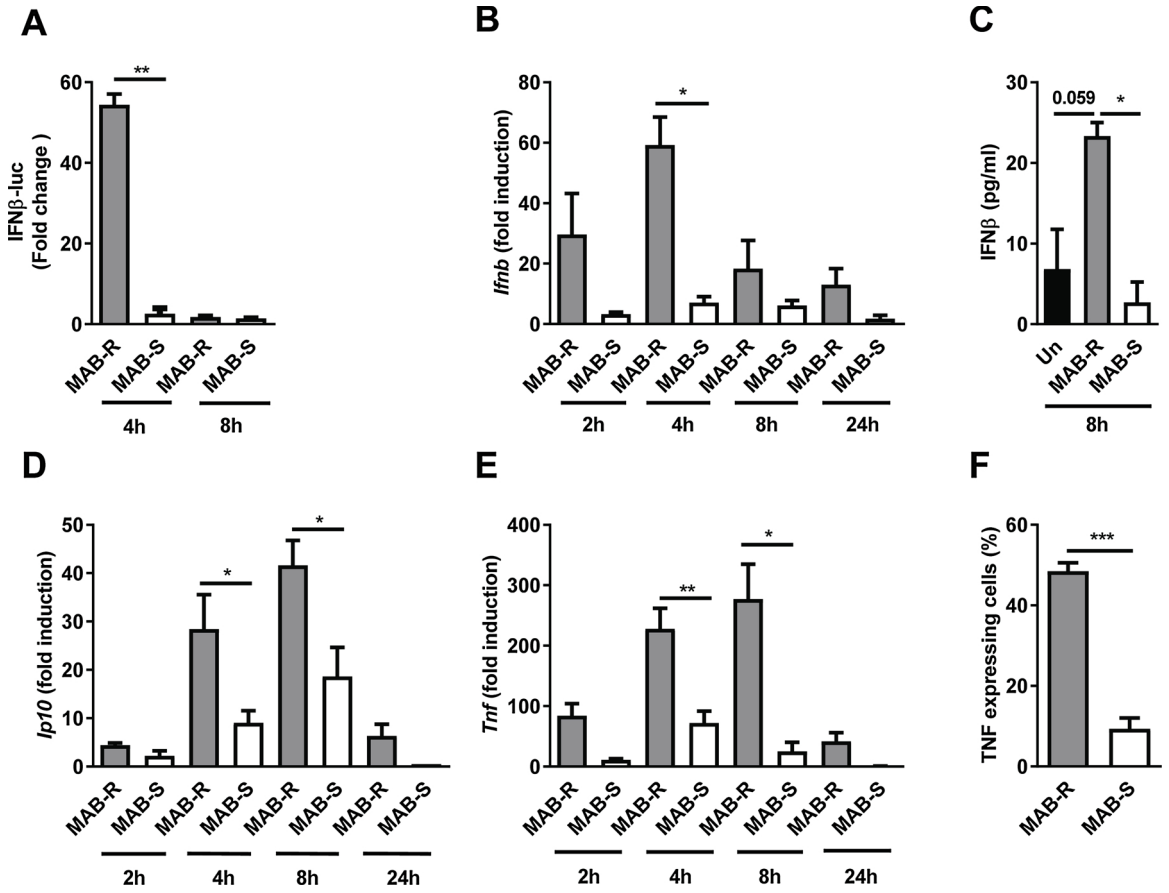

Fig. 3. Induction of IFN-β upon MABa infection in BMDM. (A) IFNβ promoter activity of BMDM_IFNβ-luc infected with MAB-R, MAB-S. Fold change values were normalized to un-infected control. (B) qRT-PCR for *Ifnb* in BMDM infected with MAB-R or MAB-S normalized to un-infected control. (C) IFNβ ELISA of supernatants from BMDM infected with MAB-R or MAB-S at 8 h p.i. (D) qRT-PCR for *Ip10* and (E) *Tnf* expression in BMDM infected with MAB-R or MAB-S. Fold change values were normalized to un-infected control. (F) Percentage of TNF producing BMDM infected with MAB-R or MAB-S for 4 h analyzed by FACS. Data are presented as mean ± SEM from at least 3 independent experiments. Statistical differences between two groups and among three groups were analyzed by 2 tailed Student's *t*-test and one way ANOVA respectively. *p < 0.05, ** < 0.01, ***p < 0.001.

understand whether differential *Ifnb* expression triggered by MAB-R and MAB-S has effects on the intrinsic ability of infected macrophages to control mycobacterial growth, we first tested if NO is produced by MAB infected macrophages. Indeed, *Nos2* and NO were produced to a higher extent in MAB-R infected macrophages than MAB-S infected macrophages, which indicated a correlation with the IFNβ expression level (Fig. 6 A and B). Next, to test if IFN-I signaling was responsible for increased NO production, WT and IFNAR$^{-/-}$ macrophages were infected with MAB-R and MAB-S and *Nos2* expression was monitored by qRT-PCR. Absence of IFNAR led to lower *Nos2* expression and nitrite level in the culture supernatants (Fig. 6C and D) of macrophages infected with MAB-R. This indicated that IFNβ produced by MAB infected macrophages and IFNAR signaling is necessary for NO production.

IFN-I are required to control NTM infections (Kuchtey et al., 2006; Ruangkiattikul et al., 2017) and additionally, NO plays an important role in restricting mycobacterial infection (Pahari et al., 2016; Zwaferink et al., 2008). Therefore, to test if IFN-I signaling and NO is required for controlling MAB infection, intracellular bacterial viabilities were determined in WT, IFNAR$^{-/-}$ and NOS2$^{-/-}$ BMDM. Due to the different internalization rate, the number of intracellular bacteria at 2 h p.i. was set to 100%. MAB-S was capable of replicating moderately inside macrophages while the growth of MAB-R was restricted in WT-BMDM (Fig. 6E). IFNAR$^{-/-}$ BMDM harbored a significantly higher number of intracellular bacteria than the WT BMDM at 48 h and 72 h in both MAB-R and MAB-S infected groups (Fig. 6E). Absence of *Nos2* also promoted the intracellular viability of both MAB strains (Fig. 6F). These results indicate that IFN-I signaling and stimulation of NO enable host cells to control intracellular MAB.

Taken together, these results clearly indicate that IFN-I signaling contributes to the clearance of MAB. Activation of IFN-I signaling upon MAB-R infection consequently induces NO production which is beneficial for the host cell to control the infection. In contrast, MAB-S stimulates a moderate IFN-I response which favors persistence inside macrophages.

4. Discussion

IFN-I seem to be important in controlling bacterial infections of patients with CF (Kormann et al., 2017; Yaacoby-Bianu et al., 2018). Though MAB is increasingly found in CF patients and often responsible for disease exacerbation, the knowledge about IFN-I in MAB infections is still incomplete. In the present study, we characterized an R-type MAB isolate from a patient with CF (MAB-R). We observed that MAB-R induced more IFNβ and TNF after infection of murine macrophages than the S-type ATCC reference strain (MAB-S). We demonstrate that IFNβ is exclusively induced via TLR2-TLR4-MyD88-TRIF-IRF3 dependent pathways upon MAB-R infection. Additionally, we show that IFN-I most probably in collaboration with TNF enhanced the intrinsic capability of macrophages to effectively clear MAB infection by inducing NOS2 activity and NO production.

It is well known that IFN-I are important for the host defense against mycobacterial infections (Denis, 1991; Kuchtey et al., 2006; Moreira-Teixeira et al., 2016; Ruangkiattikul et al., 2017; Zarogoulidis et al., 2012). However the role of IFN-I is two edged. The time point and the

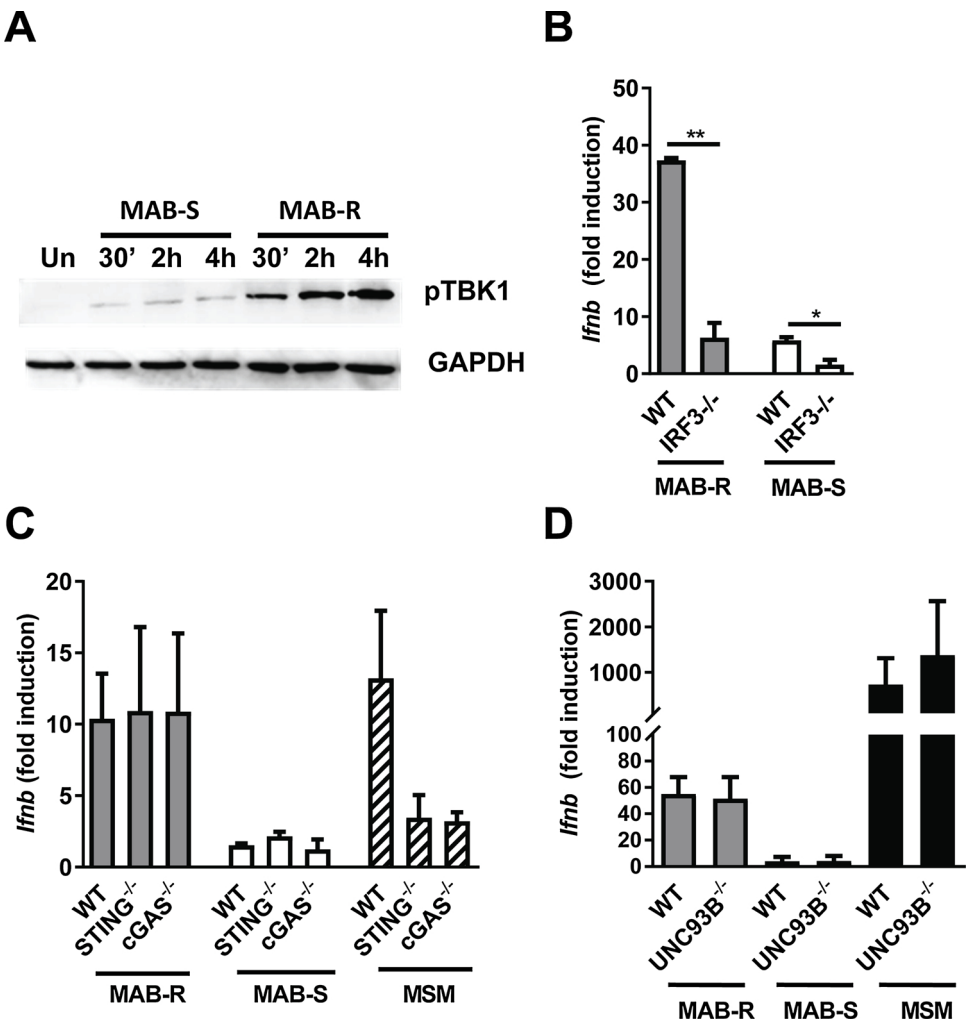

Fig. 4. MAB-R and MAB-S required TBK1 phosphorylation and IRF3 for *Ifnb* expression but the expression was independent of Sting and cGAS. (A) Immunoblot of phospho TBK1 in BMDM infected with MAB-R and MAB-S at 4 h p.i. (B) qRT-PCR for *Ifnb* in BMDM from WT compared with IRF3$^{-/-}$, (C) STING$^{-/-}$ and cGAS$^{-/-}$, (D) UNC93B$^{-/-}$. BMDM were infected with MAB-R or MAB-S for 4 h. Fold change values were normalized to un-infected control. Data are presented as mean ± SEM from at least 3 independent experiments. *p < 0.05, ** < 0.01, by 2 tailed Student's *t*-test.

extent of IFN-I activation and most probably other factors seem to determine whether IFN-I contribute to successful bacterial clearing or to exacerbation of disease (Moreira-Teixeira et al., 2018). In MTB infected macrophages IFN-I production depends to a major extent on intracellular bacterial eDNA induced cGAS-STING-TBK1-IRF3 signaling (Manzanillo et al., 2012; Watson et al., 2015). Nevertheless, involvement of TLR (Jang et al., 2018) and more recently released bacterial RNA have been shown to contribute to IFN-I production (Cheng and Schorey, 2018). Similarly, we could show that the expression of IFNβ induced by different NTM species via the cGAS-STING-TBK1-IRF3 signaling pathway requires bacterial viability and is regulated by the amount of bacterial eDNA released from the phagosome (Ruangkiattikul et al., 2017). In the present study, we show that cGAS and STING are not required for the IFN-β expression upon infection of macrophages with MAB (Fig. 4C). In addition, IFN-β induction was triggered independent of bacterial uptake excluding any involvement of intracellular signaling cascades (Fig. 5C). Rather, induction of IFN-β by MAB-R required activation of TLR2-TLR4-MyD88-TRIF-IRF3 dependent pathways. Whereas IFN-I induction by MTB requires both TLR and cGAS-STING signaling (Collins et al., 2015; Jang et al., 2018; Wassermann et al., 2015), the induction of IFN-β in MAB infected macrophages appears to be restricted to TLR signaling pathway. TLR4-TRIF and TLR2-MyD88 mediated IFNβ induction is also known for MTB, but recent works reported that the activation of TLR4-TRIF or TLR2-MyD88 induced IFNβ production differed between MTB strains (Carmona et al., 2013; Jang et al., 2018). Overall, MAB induced signaling for IFN-I induction is different from other mycobacteria.

Here we show that the extent of IFNβ production by MAB infected macrophages differed between a rough and a smooth MAB colony morphotype. The conversion from MAB S-type to R-type colony variants is attributed to a loss in GLP production (Nessar et al., 2011). Accordingly, we could identify mutations in several GLP synthesis genes of MAB-R. The consequence of such a phenotypic change is a reorganization of the outer layers of the MAB cell envelope unmasking TLR2 ligands, such as lipoproteins (Roux et al., 2011; Ryan and Byrd, 2018). By this, R-type MAB strains are more potent inducers of TNF and IL-8 (Rhoades et al., 2009; Roux et al., 2011). In agreement, our findings reveal that MAB-R induced high amounts of IFNβ and TNF. Moreover, we show that besides lipoproteins that signal via TLR2, MAB-R must express heat stable ligands triggering TLR4 dependent *Ifnb* induction. One candidate might be MAB2560 (Lee et al., 2014). Nevertheless, future studies are needed to identify the factors of MAB-R involved in pro-inflammatory signaling.

IFN-I are characterized as significant determinants of NOS2 expression thereby contributing to disease outcome during infection (Bachmann et al., 2017; Pahari et al., 2016). In the present study we could detect increased numbers of MAB-R and MAB-S in IFNAR$^{-/-}$ and NOS2$^{-/-}$ macrophages (Fig. 6E and F). Furthermore, *Nos2* expression

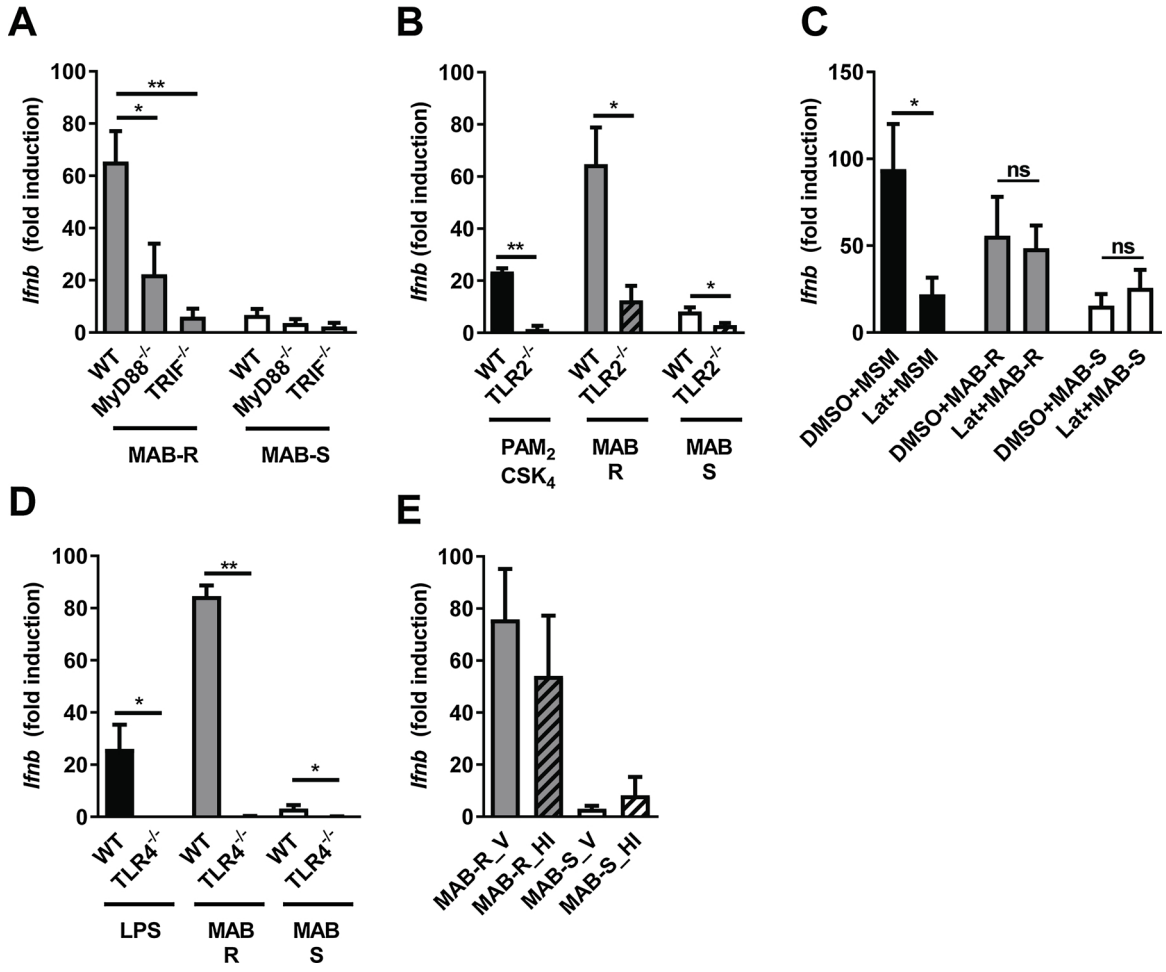

Fig. 5. MAB-R and MAB-S induce *Ifnb* expression via TLR2-TLR4-MyD88-TRIF-TBK1-IRF3 signaling pathway. (A) qRT-PCR for *Ifnb* expression in WT, MyD88$^{-/-}$ and TRIF$^{-/-}$ BMDM infected with MAB-R or MAB-S for 4 h. (B) qRT-PCR for *Ifnb* expression in WT and TLR2$^{-/-}$ BMDM infected with MAB-R or MAB-S for 4 h. (C) qRT-PCR for in BMDM pretreated with 5μM latrunculin B (Lat) for 1 h and subsequently infected with MAB-R or MAB-S for 4 h. (D) qRT-PCR for *Ifnb* expression in WT and TLR4$^{-/-}$ BMDM infected with MAB-R or MAB-S for 4 h. (E) qRT-PCR for in BMDM infected with viable (V) and heat-inactivated (HI) bacteria at 4 h p.i. Fold change values were normalized to un-infected control. Data are presented as mean ± SEM from at least 3 independent experiments. Statistical differences between two groups and among three groups were analyzed by 2 tailed Student's *t*-test and one way ANOVA respectively. *p < 0.05, ** < 0.01.

was significantly reduced and NO production was completely abolished in MAB infected IFNAR$^{-/-}$ macrophages. This clearly indicates a particular autocrine contribution of IFN-I to NO mediated restriction of MAB growth by the infected macrophage. These observations are consistent with previous studies reporting that NO was required for the restriction of MAB (Lee et al., 2017; Yaacoby-Bianu et al., 2018) and MTB infection (MacMicking et al., 1997). Nevertheless, we cannot exclude that other IFN-I dependent antimicrobial mechanisms might be additionally involved.

A striking finding of our study was the differential response of MAB-R and MAB-S to NO. As MAB-R belongs to the cluster of highly virulent MAB strains suggested to spread in the population of patients with CF (Bryant et al., 2016), it was not unexpected to observe a strong pro-inflammatory response in the infected macrophages indicated by highly induced IFNβ and TNF. Surprisingly, this response led to bacterial killing via NO. By contrast, MAB-S was less pro-inflammatory and a lower amount of NO seems to promote its persistence in WT BMDM. Overall these results are consistent with the dogma that high level of NO is toxic towards bacteria, but low, nontoxic levels of NO might support bacterial persistence by inducing bacterial dormancy through the dormancy survival regulator (Pacl et al., 2018; Voskuil et al., 2003). Therefore, in IFNAR$^{-/-}$ macrophages MAB-S was relieved from entering the NO induced dormancy stage and able to proliferate (Fig. 6E).

R-type MAB strains have been claimed hypervirulent due to their ability to stimulate strong pro-inflammatory host immune response in infection models with human or murine macrophages or infected mice (Ryan and Byrd, 2018). In addition, it was shown that clumps or cording increases virulence of MAB in a zebrafish model of infection (Bernut et al., 2014). Several studies showed that R-type MAB strains persist or grow in human monocytes while S-type MAB strains persist or declined in number (Byrd and Lyons, 1999; Howard et al., 2006; Rhoades et al., 2009; Roux et al., 2016). Those observations seem to be inconsistent with the findings shown here, i.e. MAB-R was unable to survive in murine BMDM while the MAB-S persisted. However, in contrast to mouse macrophages or human macrophages in and from people with infectious and inflammatory disease, human macrophage lines such as THP-1 as well as human blood derived primary macrophages exhibit little or no expression of NOS2 and generate little NO in response to potent inflammatory stimuli (Nathan, 2006; Thomas and Mattila, 2014). This most likely explains the observed differences.

In the presented study we observed rapid clump formation for MAB-R upon inoculation of single bacteria into the macrophage cell culture medium. However, those clumps did not influence the viability of the infected macrophages which is different from macrophages which were exposed to clumps formed in bacterial culture (Brambilla et al., 2016). Therefore the different culture procedure and MOI or macrophage infection protocol used by us may additionally account for differences to other studies. Differences in mycobacterial uptake (up to one log 10

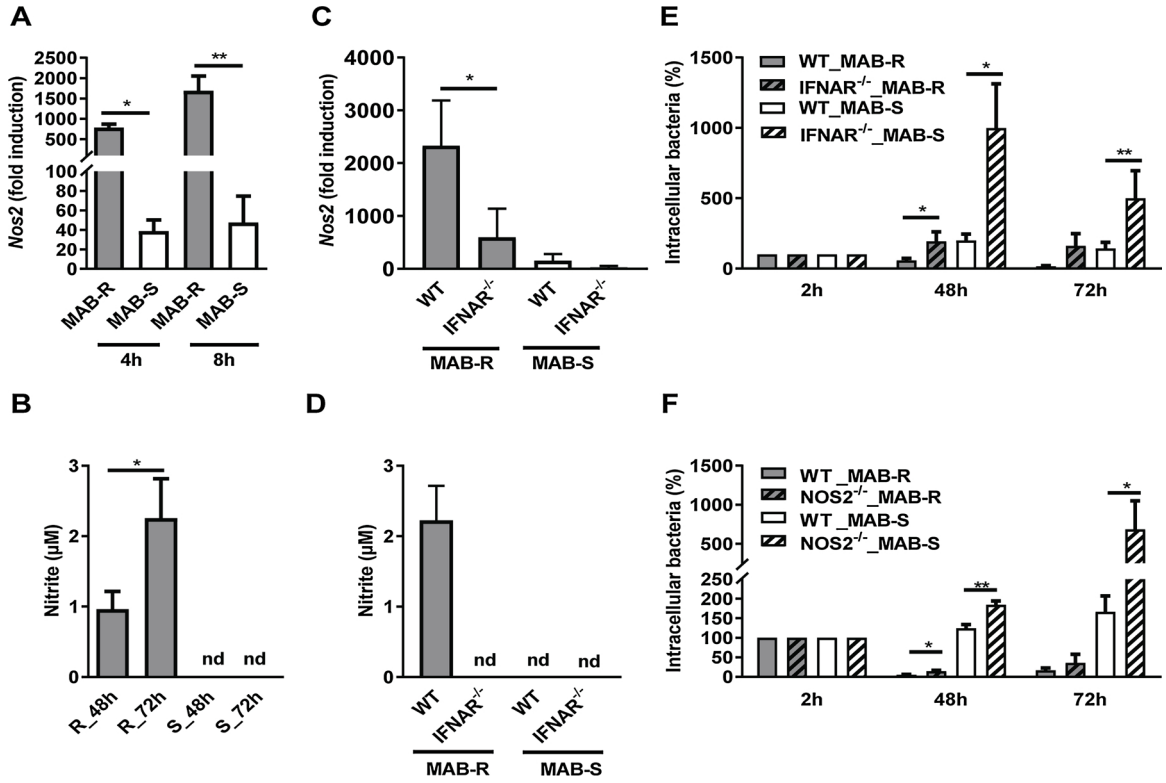

Fig. 6. IFN-I signaling is required for the induction of *Nos2* and NO and to control intracellular bacteria. (A) qRT-PCR for *Nos2* expression in BMDM_WT infected with MAB-R or MAB-S for 4 h and 8 h. Fold change values were normalized to un-infected control. (B) Nitrite levels were determined from the supernatants of BMDM infected with MAB-R (R) or MAB-S (S) at 48 and 72 h p.i. using the Griess assay. (C) qRT-PCR for *Nos2* expression in WT and IFNAR$^{-/-}$ BMDM at 4 h p.i. Fold change values were normalized to un-infected control. (D) Nitrite level in the supernatants of BMDM_WT and IFNAR$^{-/-}$ at 72 h p.i. using the Griess assay. (E) Intracellular bacterial numbers in WT and IFNAR$^{-/-}$ BMDM_and (F) WT and NOS2$^{-/-}$ BMDM_referring to 2 h p.i. as 100%. Data are presented as mean ± SEM from at least 2 independent experiments. nd, non-detectable level. *p < 0.05, ** < 0.01, by 2 tailed Student's *t*-test.

difference for the MAB-R) were observed in other macrophage infection studies with MAB (Brambilla et al., 2016; Roux et al., 2016) or *M. smegmatis* (Etienne et al., 2002) due to the loss of GPL. In agreement, as shown in Fig. 2, macrophages were more efficient in taking up MAB-R than MAB-S. Therefore, we considered the uptake rate of the two strains for calculating the survival rates. Furthermore, we calculated the survival by referring the CFU at the analyzed time points to the bacterial CFU at 2 h pi.. In our hands this procedure allows a better comparison of the survival of MAB-R and MAB-S.

S-type MAB strains seem to exhibit the same trait as slow growing pathogenic mycobacteria such as restriction of endosome acidification and low induction of apoptosis and autophagy (Roux et al., 2016). Here we show that they also induce less IFNβ which might favor their persistence in the host as shown for other pathogenic NTM (Ruangkiattikul et al., 2017). In addition, we propose that the strong immune activation does not correlate with virulence. On the macrophage level, our data clearly indicate that MAB-R is less virulent than MAB-S. Therefore, MAB-R behaves similarly to other non-pathogenic rapid growing mycobacteria e.g. *M. smegmatis* and *M. fortuitum*, the strong cytokine response is linked to clearing of infection (Bohsali et al., 2010; Ruangkiattikul et al., 2017). Thus, strong IFN-β expression, as well as that of other pro-inflammatory cytokines in MAB infections, could be inversely correlated to the bacterial virulence and persistence. Therefore dysfunctions in IFN-I production might explain the presence of R-type MAB strains in patients with CF.

IFN-I have a central role in the initiation of the inflammatory response of the lung (Makris et al., 2017). Correspondingly, transcriptomic profiling revealed enriched IFN-I mRNA expression in patients with mild CF and low IFN-I mRNA expression in patients with severe CF, addressing the role of IFN-I in the severity of disease (Kormann et al., 2017). Therefore, hypothetically, in patients with mild CF, R-type MAB strains should be cleared by the host while patients with severe CF might be unable to control infection. In accordance, the clinical disease progression of MAB-R donor patient described here is very unfavorable and characterized by decreasing lung function and accumulation of bacterial and fungal pathogens in the lung. S-type MAB strains might persist in all patients with CF. In fact, both R-type and S-type MAB strains could be isolated from the patients with mild and severe CF and R-type strains are more often isolated (Catherinot et al., 2013; Pawlik et al., 2013; Qvist et al., 2015; Ruger et al., 2014). Our results suggest that the reasons for this could be due to a general impairment of IFN-I production caused, for example, by the dysfunction of CFTR in airway epithelial cells in patients with CF (Parker et al., 2012) or an inefficient induction of TLR4-IFN-I signaling as a consequence of decreased TLR4 expression in CF airway cells (John et al., 2010). This might protect R-type strains from being killed by macrophages. Indeed, recently, treatment of patients with CF with NO inhalation showed a significant reduction of MAB number in sputum (Yaacoby-Bianu et al., 2018) indicating that MAB is susceptible to NO but the endogenous NO production by the CF host is inefficient to combat the MAB infection. Correspondingly, it was shown that TLR2 is necessary for an early protective Th1 response in mice, infected with R-type MAB, (Kim et al., 2015a) and a case report demonstrated that inhalation of the macrophage activator granulocyte–macrophage colony-stimulating factor resulted in decreased MAB burden in patients with CF (Scott et al., 2018).

In conclusion, our data demonstrate that IFN-I signaling is necessary to control MAB infections. The persistence of MAB in macrophages is determined by its ability to activate IFN-β via the TLR2-TLR4-MyD88-TRIF-IRF3 axis. This leads to the up-regulation of *Nos2* expression and NO production which help to control infection. Our data suggest that persistence of MAB infections in CF patients might be due to a restricted IFN-I response. Understanding these pathways may help in the

development of future strategies to stimulate host macrophage activity to treat MAB infected patients more effectively.

Conflict of interest

The authors declare that there are no conflicts of interest regarding the publication of this paper.

Author contribution

Designed experiments: NR CS AL RG; performed the experiments: NR DR KA MR TS PT; analyzed the data: NR UK TS CS AL RG; wrote the manuscript: NR AL RG

Acknowledgment

We thank Siegfried Weiß (Helmholtz Centre for Infection Research, Braunschweig, Germany) for providing TLR2$^{-/-}$ mice and Stefan Lienenklaus (Institute for Experimental Infection Research, TWINCORE, Hannover, Germany) for providing IFN-β$^{+/\Delta\beta\text{-luc}}$ mice. We are grateful to Melanie Brinkmann (Helmholtz Centre for Infection Research, Braunschweig, Germany) for providing the UNC93B$^{-/-}$ and Charles M. Rice (Rockefeller University, New York, USA) for providing cGAS$^{-/-}$ mice. We thank Martin Reichel and Felix Knauf (Medizinische Klinik m. S. Nephrologie und Internistische Intensivmedizin, Charité - Universitätsmedizin Berlin, Germany) for providing bones from TLR4$^{-/-}$ mice and Ulrike Schleicher und Christian Bogdan (Mikrobiologisches Institut – Klinische Mikrobiologie, Immunologie und Hygiene, Friedrich-Alexander-Universität Erlangen-Nürnberg, Universitätsklinikum Erlangen, Erlangen, Germany) for bones from NOS2$^{-/-}$ mice. We further acknowledge the NGS support unit (MF2) of the Robert Koch Institute for whole genome sequencing and Elisabeth Kamal (Robert Koch Institute) and Kristin Laarmann (University of Veterinary Medicine Hannover) for excellent technical assistance. This work was supported by a grant from the German Research Foundation (DFG, Go983/4-1) to RG and by an award of the German “Gilead Förderprogramm Infektiologie 2018” to CS. The funders had no role in study design, data collection and interpretation, or the decision to submit the work for publication.

Appendix A. Supplementary data

Supplementary material related to this article can be found, in the online version, at doi:https://doi.org/10.1016/j.ijmm.2019.05.007.

References

Andrade, W.A., Firon, A., Schmidt, T., Hornung, V., Fitzgerald, K.A., Kurt-Jones, E.A., Trieu-Cuot, P., Golenbock, D.T., Kaminski, P.A., 2016. Group B Streptococcus Degrades Cyclic-di-AMP to modulate STING-Dependent type I interferon production. Cell Host Microbe 20, 49–59.

Bachmann, M., Waibler, Z., Pleli, T., Pfeilschifter, J., Muhl, H., 2017. Type I interferon supports inducible nitric oxide synthase in murine hepatoma cells and hepatocytes and during experimental acetaminophen-induced liver damage. Front. Immunol. 8, 890.

Bankevich, A., Nurk, S., Antipov, D., Gurevich, A.A., Dvorkin, M., Kulikov, A.S., Lesin, V.M., Nikolenko, S.I., Pham, S., Prjibelski, A.D., Pyshkin, A.V., Sirotkin, A.V., Vyahhi, N., Tesler, G., Alekseyev, M.A., Pevzner, P.A., 2012. SPAdes: a new genome assembly algorithm and its applications to single-cell sequencing. J. Comput. Biol. 19, 455–477.

Bernut, A., Herrmann, J.L., Kissa, K., Dubremetz, J.F., Gaillard, J.L., Lutfalla, G., Kremer, L., 2014. Mycobacterium abscessus cording prevents phagocytosis and promotes abscess formation. Proc. Natl. Acad. Sci. U. S. A. 111, E943–952.

Bogdan, C., 2015. Nitric oxide synthase in innate and adaptive immunity: an update. Trends Immunol. 36, 161–178.

Bohsali, A., Abdalla, H., Velmurugan, K., Briken, V., 2010. The non-pathogenic mycobacteria M. smegmatis and M. fortuitum induce rapid host cell apoptosis via a caspase-3 and TNF dependent pathway. BMC Microbiol. 10, 237.

Borden, E.C., Sen, G.C., Uze, G., Silverman, R.H., Ransohoff, R.M., Foster, G.R., Stark, G.R., 2007. Interferons at age 50: past, current and future impact on biomedicine. Nat. Rev. Drug Discov. 6, 975–990.

Boxx, G.M., Cheng, G., 2016. The roles of type I interferon in bacterial infection. Cell Host Microbe 19, 760–769.

Brambilla, C., Llorens-Fons, M., Julian, E., Noguera-Ortega, E., Tomas-Martinez, C., Perez-Trujillo, M., Byrd, T.F., Alcaide, F., Luquin, M., 2016. Mycobacteria clumping increase their capacity to damage macrophages. Front. Microbiol. 7, 1562.

Bryant, J.M., Grogono, D.M., Rodriguez-Rincon, D., Everall, I., Brown, K.P., Moreno, P., Verma, D., Hill, E., Drijkoningen, J., Gilligan, P., Esther, C.R., Noone, P.G., Giddings, O., Bell, S.C., Thomson, R., Wainwright, C.E., Coulter, C., Pandey, S., Wood, M.E., Stockwell, R.E., Ramsay, K.A., Sherrard, L.J., Kidd, T.J., Jabbour, N., Johnson, G.R., Knibbs, L.D., Morawska, L., Sly, P.D., Jones, A., Bilton, D., Laurenson, I., Ruddy, M., Bourke, S., Bowler, I.C., Chapman, S.J., Clayton, A., Cullen, M., Daniels, T., Dempsey, O., Denton, M., Desai, M., Drew, R.J., Edenborough, F., Evans, J., Folb, J., Humphrey, H., Isalska, B., Jensen-Fangel, S., Jonsson, B., Jones, A.M., Katzenstein, T.L., Lillebaek, T., MacGregor, G., Mayell, S., Millar, M., Modha, D., Nash, E.F., O'Brien, C., O'Brien, D., Ohri, C., Pao, C.S., Peckham, D., Perrin, F., Perry, A., Pressler, T., Prtak, L., Qvist, T., Robb, A., Rodgers, H., Schaffer, K., Shafi, N., van Ingen, J., Walshaw, M., Watson, D., West, N., Whitehouse, J., Haworth, C.S., Harris, S.R., Ordway, D., Parkhill, J., Floto, R.A., 2016. Emergence and spread of a human-transmissible multidrug-resistant nontuberculous mycobacterium. Science 354, 751–757.

Byrd, T.F., Lyons, C.R., 1999. Preliminary characterization of a Mycobacterium abscessus mutant in human and murine models of infection. Infect. Immun. 67, 4700–4707.

Carmona, J., Cruz, A., Moreira-Teixeira, L., Sousa, C., Sousa, J., Osorio, N.S., Saraiva, A.L., Svenson, S., Kallenius, G., Pedrosa, J., Rodrigues, F., Castro, A.G., Saraiva, M., 2013. Mycobacterium tuberculosis strains are differentially recognized by TLRs with an impact on the immune response. PLoS One 8, e67277.

Catherinot, E., Roux, A.L., Vibet, M.A., Bellis, G., Ravilly, S., Lemonnier, L., Le Roux, E., Bernede-Bauduin, C., Le Bourgeois, M., Herrmann, J.L., Guillemot, D., Gaillard, J.L., group, O.M.A., 2013. Mycobacterium avium and Mycobacterium abscessus complex target distinct cystic fibrosis patient subpopulations. J. Cyst. Fibros. 12, 74–80.

Chan, E.D., Chan, J., Schluger, N.W., 2001. What is the role of nitric oxide in murine and human host defense against tuberculosis?Current knowledge. Am. J. Respir. Cell Mol. Biol. 25, 606–612.

Cheng, Y., Schorey, J.S., 2018. Mycobacterium tuberculosis-induced IFN-beta production requires cytosolic DNA and RNA sensing pathways. J. Exp. Med.

Choi, G.E., Chang, C.L., Whang, J., Kim, H.J., Kwon, O.J., Koh, W.J., Shin, S.J., 2011. Efficient differentiation of Mycobacterium abscessus complex isolates to the species level by a novel PCR-based variable-number tandem-repeat assay. J. Clin. Microbiol. 49, 1107–1109.

Collins, A.C., Cai, H., Li, T., Franco, L.H., Li, X.D., Nair, V.R., Scharn, C.R., Stamm, C.E., Levine, B., Chen, Z.J., Shiloh, M.U., 2015. Cyclic GMP-AMP synthase is an innate immune DNA sensor for Mycobacterium tuberculosis. Cell Host Microbe 17, 820–828.

Coscolla, M., Lewin, A., Metzger, S., Maetz-Rennsing, K., Calvignac-Spencer, S., Nitsche, A., Dabrowski, P.W., Radonic, A., Niemann, S., Parkhill, J., Couacy-Hymann, E., Feldman, J., Comas, I., Boesch, C., Gagneux, S., Leendertz, F.H., 2013. Novel Mycobacterium tuberculosis complex isolate from a wild chimpanzee. Emerg. Infect. Dis. 19, 969–976.

Costa, V.M., Torres, K.C., Mendonca, R.Z., Gresser, I., Gollob, K.J., Abrahamsohn, I.A., 2006. Type I IFNs stimulate nitric oxide production and resistance to Trypanosoma cruzi infection. J. Immunol. 177, 3193–3200.

Denis, M., 1991. Recombinant murine beta interferon enhances resistance of mice to systemic Mycobacterium avium infection. Infect. Immun. 59, 1857–1859.

Dietrich, N., Lienenklaus, S., Weiss, S., Gekara, N.O., 2010. Murine toll-like receptor 2 activation induces type I interferon responses from endolysosomal compartments. PLoS One 5, e10250.

Etienne, G., Villeneuve, C., Billman-Jacobe, H., Astarie-Dequeker, C., Dupont, M.A., Daffe, M., 2002. The impact of the absence of glycopeptidolipids on the ultrastructure, cell surface and cell wall properties, and phagocytosis of Mycobacterium smegmatis. Microbiology 148, 3089–3100.

Frau, J., Cossu, D., Coghe, G., Lorefice, L., Fenu, G., Porcu, G., Sardu, C., Murru, M.R., Tranquilli, S., Marrosu, M.G., Sechi, L.A., Cocco, E., 2015. Role of interferon-beta in Mycobacterium avium subspecies paratuberculosis antibody response in Sardinian MS patients. J. Neurol. Sci. 349, 249–250.

Hansen, K., Prabakaran, T., Laustsen, A., Jorgensen, S.E., Rahbaek, S.H., Jensen, S.B., Nielsen, R., Leber, J.H., Decker, T., Horan, K.A., Jakobsen, M.R., Paludan, S.R., 2014. Listeria monocytogenes induces IFNbeta expression through an IFI16-, cGAS- and STING-dependent pathway. EMBO J. 33, 1654–1666.

Howard, S.T., Rhoades, E., Recht, J., Pang, X., Alsup, A., Kolter, R., Lyons, C.R., Byrd, T.F., 2006. Spontaneous reversion of Mycobacterium abscessus from a smooth to a rough morphotype is associated with reduced expression of glycopeptidolipid and reacquisition of an invasive phenotype. Microbiology 152, 1581–1590.

Huys, L., Van Hauwermeiren, F., Dejager, L., Dejonckheere, E., Lienenklaus, S., Weiss, S., Leclercq, G., Libert, C., 2009. Type I interferon drives tumor necrosis factor-induced lethal shock. J. Exp. Med. 206, 1873–1882.

Jacobs, A.T., Ignarro, L.J., 2001. Lipopolysaccharide-induced expression of interferon-beta mediates the timing of inducible nitric-oxide synthase induction in RAW 264.7 macrophages. J. Biol. Chem. 276, 47950–47957.

Jang, A.R., Choi, J.H., Shin, S.J., Park, J.H., 2018. Mycobacterium tuberculosis ESAT6 induces IFN-beta gene expression in Macrophages via TLRs-mediated signaling. Cytokine 104, 104–109.

John, G., Yildirim, A.O., Rubin, B.K., Gruenert, D.C., Henke, M.O., 2010. TLR-4-mediated innate immunity is reduced in cystic fibrosis airway cells. Am. J. Respir. Cell Mol. Biol. 42, 424–431.

Jonsson, B.E., Gilljam, M., Lindblad, A., Ridell, M., Wold, A.E., Welinder-Olsson, C., 2007. Molecular epidemiology of Mycobacterium abscessus, with focus on cystic fibrosis. J. Clin. Microbiol. 45, 1497–1504.

Kim, J.S., Kang, M.J., Kim, W.S., Han, S.J., Kim, H.M., Kim, H.W., Kwon, K.W., Kim, S.J.,

Cha, S.B., Eum, S.Y., Koh, W.J., Cho, S.N., Park, J.H., Shin, S.J., 2015a. Essential engagement of Toll-like receptor 2 in initiation of early protective Th1 response against rough variants of Mycobacterium abscessus. Infect. Immun. 83, 1556–1567.
Kim, M.H., Kim, Y.H., Kang, S.Y., Lee, W.I., 2015b. The incidence of non-tuberculous Mycobacterium lung disease in patients with suspected pulmonary tuberculosis. Indian J. Microbiol. 55, 464–468.
Kormann, M.S.D., Dewerth, A., Eichner, F., Baskaran, P., Hector, A., Regamey, N., Hartl, D., Handgretinger, R., Antony, J.S., 2017. Transcriptomic profile of cystic fibrosis patients identifies type I interferon response and ribosomal stalk proteins as potential modifiers of disease severity. PLoS One 12, e0183526.
Kuchtey, J., Fulton, S.A., Reba, S.M., Harding, C.V., Boom, W.H., 2006. Interferon-alphabeta mediates partial control of early pulmonary Mycobacterium bovis bacillus Calmette-Guerin infection. Immunology 118, 39–49.
Kuehnel, M.P., Goethe, R., Habermann, A., Mueller, E., Rohde, M., Griffiths, G., Valentin-Weigand, P., 2001. Characterization of the intracellular survival of Mycobacterium avium ssp. paratuberculosis: phagosomal pH and fusogenicity in J774 macrophages compared with other mycobacteria. Cell. Microbiol. 3, 551–566.
Lee, J.Y., Lee, M.S., Kim, D.J., Yang, S.J., Lee, S.J., Noh, E.J., Shin, S.J., Park, J.H., 2017. Nucleotide-binding oligomerization domain 2 contributes to limiting growth of Mycobacterium abscessus in the lung of mice by regulating cytokines and nitric oxide production. Front. Immunol. 8, 1477.
Lee, M.R., Sheng, W.H., Hung, C.C., Yu, C.J., Lee, L.N., Hsueh, P.R., 2015. Mycobacterium abscessus complex infections in humans. Emerg Infect. Dis. 21, 1638–1646.
Lee, S.J., Shin, S.J., Lee, S.J., Lee, M.H., Kang, T.H., Noh, K.T., Shin, Y.K., Kim, H.W., Yun, C.H., Jung, I.D., Park, Y.M., 2014. Mycobacterium abscessus MAB2560 induces maturation of dendritic cells via Toll-like receptor 4 and drives Th1 immune response. BMB Rep. 47, 512–517.
Lienenklaus, S., Cornitescu, M., Zietara, N., Lyszkiewicz, M., Gekara, N., Jablonska, J., Edenhofer, F., Rajewsky, K., Bruder, D., Hafner, M., Staeheli, P., Weiss, S., 2009. Novel reporter mouse reveals constitutive and inflammatory expression of IFN-beta in vivo. J. Immunol. 183, 3229–3236.
MacMicking, J.D., North, R.J., LaCourse, R., Mudgett, J.S., Shah, S.K., Nathan, C.F., 1997. Identification of nitric oxide synthase as a protective locus against tuberculosis. Proc. Natl. Acad. Sci. U. S. A. 94, 5243–5248.
Makris, S., Paulsen, M., Johansson, C., 2017. Type I interferons as regulators of lung inflammation. Front. Immunol. 8, 259.
Manzanillo, P.S., Shiloh, M.U., Portnoy, D.A., Cox, J.S., 2012. Mycobacterium tuberculosis activates the DNA-dependent cytosolic surveillance pathway within macrophages. Cell Host Microbe 11, 469–480.
Moeller, A., Horak Jr., F., Lane, C., Knight, D., Kicic, A., Brennan, S., Franklin, P., Terpolilli, J., Wildhaber, J.H., Stick, S.M., 2006. Inducible NO synthase expression is low in airway epithelium from young children with cystic fibrosis. Thorax 61, 514–520.
Moreira-Teixeira, L., Mayer-Barber, K., Sher, A., O'Garra, A., 2018. Type I interferons in tuberculosis: foe and occasionally friend. J. Exp. Med. 215, 1273–1285.
Moreira-Teixeira, L., Sousa, J., McNab, F.W., Torrado, E., Cardoso, F., Machado, H., Castro, F., Cardoso, V., Gaifem, J., Wu, X., Appelberg, R., Castro, A.G., O'Garra, A., Saraiva, M., 2016. Type I IFN inhibits alternative macrophage activation during Mycobacterium tuberculosis infection and leads to enhanced protection in the absence of IFN-gamma signaling. J. Immunol. 197, 4714–4726.
Nathan, C., 2006. Role of iNOS in human host defense. Science 312, 1874–1875 author reply 1874-1875.
Nessar, R., Reyrat, J.M., Davidson, L.B., Byrd, T.F., 2011. Deletion of the mmpL4b gene in the Mycobacterium abscessus glycopeptidolipid biosynthetic pathway results in loss of surface colonization capability, but enhanced ability to replicate in human macrophages and stimulate their innate immune response. Microbiology 157, 1187–1195.
Pacl, H.T., Reddy, V.P., Saini, V., Chinta, K.C., Steyn, A.J.C., 2018. Host-pathogen redox dynamics modulate Mycobacterium tuberculosis pathogenesis. Pathog. Dis. 76.
Page, A.J., Cummins, C.A., Hunt, M., Wong, V.K., Reuter, S., Holden, M.T., Fookes, M., Falush, D., Keane, J.A., Parkhill, J., 2015. Roary: rapid large-scale prokaryote pan genome analysis. Bioinformatics 31, 3691–3693.
Pahari, S., Khan, N., Aqdas, M., Negi, S., Kaur, J., Agrewala, J.N., 2016. Infergen stimulated macrophages restrict Mycobacterium tuberculosis growth by autophagy and release of nitric oxide. Sci. Rep. 6, 39492.
Parker, D., Cohen, T.S., Alhede, M., Harfenist, B.S., Martin, F.J., Prince, A., 2012. Induction of type I interferon signaling by Pseudomonas aeruginosa is diminished in cystic fibrosis epithelial cells. Am. J. Respir. Cell Mol. Biol. 46, 6–13.
Pawlik, A., Garnier, G., Orgeur, M., Tong, P., Lohan, A., Le Chevalier, F., Sapriel, G., Roux, A.L., Conlon, K., Honore, N., Dillies, M.A., Ma, L., Bouchier, C., Coppee, J.Y., Gaillard, J.L., Gordon, S.V., Loftus, B., Brosch, R., Herrmann, J.L., 2013. Identification and characterization of the genetic changes responsible for the characteristic smooth-to-rough morphotype alterations of clinically persistent Mycobacterium abscessus. Mol. Microbiol. 90, 612–629.
Qvist, T., Gilljam, M., Jonsson, B., Taylor-Robinson, D., Jensen-Fangel, S., Wang, M., Svahn, A., Kotz, K., Hansson, L., Hollsing, A., Hansen, C.R., Finstad, P.L., Pressler, T., Hoiby, N., Katzenstein, T.L., Scandinavian Cystic Fibrosis Study, C, 2015. Epidemiology of nontuberculous mycobacteria among patients with cystic fibrosis in Scandinavia. J. Cyst. Fibros. 14, 46–52.
Rhoades, E.R., Archambault, A.S., Greendyke, R., Hsu, F.F., Streeter, C., Byrd, T.F., 2009. Mycobacterium abscessus Glycopeptidolipids mask underlying cell wall phosphatidyl-myo-inositol mannosides blocking induction of human macrophage TNF-alpha by preventing interaction with TLR2. J. Immunol. 183, 1997–2007.
Roehr, J.T., Dieterich, C., Reinert, K., 2017. Flexbar 3.0 - SIMD and multicore parallelization. Bioinformatics 33, 2941–2942.
Roux, A.L., Ray, A., Pawlik, A., Medjahed, H., Etienne, G., Rottman, M., Catherinot, E., Coppee, J.Y., Chaoui, K., Monsarrat, B., Toubert, A., Daffe, M., Puzo, G., Gaillard, J.L., Brosch, R., Dulphy, N., Nigou, J., Herrmann, J.L., 2011. Overexpression of proinflammatory TLR-2-signalling lipoproteins in hypervirulent mycobacterial variants. Cell. Microbiol. 13, 692–704.
Roux, A.L., Viljoen, A., Bah, A., Simeone, R., Bernut, A., Laencina, L., Deramaudt, T., Rottman, M., Gaillard, J.L., Majlessi, L., Brosch, R., Girard-Misguich, F., Vergne, I., de Chastellier, C., Kremer, L., Herrmann, J.L., 2016. The distinct fate of smooth and rough Mycobacterium abscessus variants inside macrophages. Open Biol. 6.
Ruangkiattikul, N., Nerlich, A., Abdissa, K., Lienenklaus, S., Suwandi, A., Janze, N., Laarmann, K., Spanier, J., Kalinke, U., Weiss, S., Goethe, R., 2017. cGAS-STING-TBK1-IRF3/7 induced interferon-beta contributes to the clearing of non tuberculous mycobacterial infection in mice. Virulence 8, 1303–1315.
Ruger, K., Hampel, A., Billig, S., Rucker, N., Suerbaum, S., Bange, F.C., 2014. Characterization of rough and smooth morphotypes of Mycobacterium abscessus isolates from clinical specimens. J. Clin. Microbiol. 52, 244–250.
Ryan, K., Byrd, T.F., 2018. Mycobacterium abscessus: shapeshifter of the mycobacterial world. Front. Microbiol. 9, 2642.
Scott, J.P., Ji, Y., Kannan, M., Wylam, M.E., 2018. Inhaled granulocyte-macrophage colony-stimulating factor for Mycobacterium abscessus in cystic fibrosis. Eur. Respir. J. 51.
Shin, S.J., Lee, B.S., Koh, W.J., Manning, E.J., Anklam, K., Sreevatsan, S., Lambrecht, R.S., Collins, M.T., 2010. Efficient differentiation of Mycobacterium avium complex species and subspecies by use of five-target multiplex PCR. J. Clin. Microbiol. 48, 4057–4062.
Stamatakis, A., 2014. RAxML version 8: a tool for phylogenetic analysis and post-analysis of large phylogenies. Bioinformatics 30, 1312–1313.
Thomas, A.C., Mattila, J.T., 2014. Of mice and men": arginine metabolism in macrophages. Front. Immunol. 5, 479.
Trinchieri, G., 2010. Type I interferon: friend or foe? J. Exp. Med. 207, 2053–2063.
Tsai, S.H., Lai, H.C., Hu, S.T., 2015. Subinhibitory doses of aminoglycoside antibiotics induce changes in the phenotype of Mycobacterium abscessus. Antimicrob. Agents Chemother. 59, 6161–6169.
Voskuil, M.I., Schnappinger, D., Visconti, K.C., Harrell, M.I., Dolganov, G.M., Sherman, D.R., Schoolnik, G.K., 2003. Inhibition of respiration by nitric oxide induces a Mycobacterium tuberculosis dormancy program. J. Exp. Med. 198, 705–713.
Wassermann, R., Gulen, M.F., Sala, C., Perin, S.G., Lou, Y., Rybniker, J., Schmid-Burgk, J.L., Schmidt, T., Hornung, V., Cole, S.T., Ablasser, A., 2015. Mycobacterium tuberculosis differentially activates cGAS- and inflammasome-dependent intracellular immune responses through ESX-1. Cell Host Microbe 17, 799–810.
Wassilew, N., Hoffmann, H., Andrejak, C., Lange, C., 2016. Pulmonary disease caused by non-tuberculous mycobacteria. Respiration 91, 386–402.
Watson, R.O., Bell, S.L., MacDuff, D.A., Kimmey, J.M., Diner, E.J., Olivas, J., Vance, R.E., Stallings, C.L., Virgin, H.W., Cox, J.S., 2015. The cytosolic sensor cGAS detects Mycobacterium tuberculosis DNA to induce type I interferons and activate autophagy. Cell Host Microbe 17, 811–819.
Yaacoby-Bianu, K., Gur, M., Toukan, Y., Nir, V., Hakim, F., Geffen, Y., Bentur, L., 2018. Compassionate nitric oxide adjuvant treatment of persistent Mycobacterium infection in cystic fibrosis patients. Pediatr. Infect. Dis. J. 37, 336–338.
Yang, K., Wu, Y., Xie, H., Li, M., Ming, S., Li, L., Li, M., Wu, M., Gong, S., Huang, X., 2016. Macrophage-mediated inflammatory response decreases mycobacterial survival in mouse MSCs by augmenting NO production. Sci. Rep. 6, 27326.
Zarogoulidis, P., Kioumis, I., Papanas, N., Manika, K., Kontakiotis, T., Papagianis, A., Zarogoulidis, K., 2012. The effect of combination IFN-alpha-2a with usual anti-tuberculosis chemotherapy in non-responding tuberculosis and diabetes mellitus: a case report and review of the literature. J. Chemother. 24, 173–177.
Zwaferink, H., Stockinger, S., Reipert, S., Decker, T., 2008. Stimulation of inducible nitric oxide synthase expression by beta interferon increases necrotic death of macrophages upon Listeria monocytogenes infection. Infect. Immun. 76, 1649–1656.